Two Tube Models of Rubber Elasticity

W. L. VANDOOLAEGHE, S. KUTTER, E. M. TERENTJEV

Cavendish Laboratory, University of Cambridge, Cambridge CB3 0HE, United Kingdom

Received 31 January 2006; revised 23 March 2006; accepted 6 April 2006
DOI: 10.1002/polb.20900
Published online in Wiley InterScience (www.interscience.wiley.com).

ABSTRACT: Polymer entanglements lead to complicated topological constraints and interactions between neighboring chains in a dense solution or melt. Entanglements can be treated in a mean field approach, within the famous reptation model, since they effectively confine each individual chain in a tube-like geometry. In polymer networks, due to crosslinks preventing the global reptation and constraint release, entanglements acquire a different topological meaning and have a much stronger effect on the resulting mechanical response. In this article we discuss two different models of rubber elasticity, both utilizing the reptation ideas. First, we apply the classical ideas of reptation statistics to calculate the effective rubber-elastic free energy of an entangled rubbery network. In the second approach, we examine the classical Rouse dynamics of chains with quenched constraints at their ends by crosslinks, and along the primitive path by entanglements. We then proceed to average a *microscopic* stress tensor for the network system and present it in a manageable form in the equilibrium $t \to \infty$ limit. Particular attention is paid to the treatment of compressibility and hydrostatic pressure in a sample with open boundaries. © 2006 Wiley Periodicals, Inc. J Polym Sci Part B: Polym Phys 44: 2679–2697, 2006
Keywords: constraints; dynamics; elastomers; entanglements; Polymers; reptation; rubber modulus

INTRODUCTION

Understanding the molecular mechanisms of rubber elasticity has remained one of the most significant unsolved problems in polymer theory. Polymer networks are highly complex disordered systems. Rubber, for example, is a macroscopic network polymer that has three-dimensional structure in which each chain is connected to all the others by a sequence of junction points, called crosslinks. The crosslinks, together with the conformational entropy arising from the chain flexibility, are responsible for rubber elasticity. This is the most basic view of a material that is expected to contain network inhomogeneities and other defects, such as trapped entanglements, which will alter its elastic behavior as well.

The simplest theoretical models consider the network as being made of *phantom* or ideal chains. Each polymer is modeled by a three-dimensional random walk in space: chains may freely intersect and the network strand conformations are assumed to be independent of one another. To form a corresponding *phantom* network, the chains are linked to each other at their end points, but do not interact otherwise, in particular, they are able to fluctuate freely between crosslinks. In a real network, the exact location of the crosslinks can vary from one specimen to the next. However, any two samples having different crosslink realizations will exhibit similar macroscopic properties. The ideal chain model, although crude, is the customary first approach when solving polymer theory problems.

If one aims to improve the phantom model, one is confronted with the complexity of entanglements

Correspondence to: E. M. Terentjev (E-mail: emt1000@cam.ac.uk)

Journal of Polymer Science: Part B: Polymer Physics, Vol. 44, 2679–2697 (2006)

and their topological constraints. The mean field treatment of entangled polymer systems is a now classical reptation theory,[1,2] which had a spectacular success in describing a large variety of different physical effects in melts and semi-dilute solutions. However, the analogous description of crosslinked rubbery networks has been much less successful. This is due to the difference in the entanglement topology: in a polymer melt the confining chain has to be long enough to form a topological knot around a chosen polymer; even then the constraint is only dynamical and can be released by a reptation diffusion along the chain path. In a crosslinked network, any loop around a chosen strand becomes an entanglement, which could be mobile but cannot be released altogether.

An early model of elastic response of entangled rubbers was developed by Edwards.[3] In tradition with the melt theory, it assumed that the presence of neighboring strands in a dense network effectively confines a particular polymer strand to a tube, whose axis defines the primitive path, see Figure 2 in "Reptation theory of rubber elasticity" later. Within this tube, the polymer is free to explore all possible configurations, performing random excursions, parallel and perpendicular to the axis of the tube. One can show that on deformation the length of the primitive path increases. Since the arc length of the polymer is constant, the amount of chain available for perpendicular excursions is reduced, leading to a reduction in entropy and hence to an increase in free energy. However, the particular calculation in ref. 4 has a number of shortcomings; perhaps, the main limitation is that one only looks at the entropy reduction associated with the overall change of primitive path contour length on deformation, ignoring the essential mechanisms of local reptation and segment re-distribution between different tube segments.

Gaylord and Douglas (GD) developed a simple *localization* model where each strand segment is placed in a virtual hard tube of a square cross-section.[5] Assuming that the deformation affinely changes the dimensions of the tube, they calculate by means of scaling arguments the change in free energy of a network, with each chain confined in such a tube. Ball et al. (BDEW) chose a completely different approach, referred to as the *slip-link* model.[6] The effect of an entanglement is modeled as a local mobile confinement site, a link between two interwound strands, which is able to slip up and down along both strands. Higgs and Ball (HB) adopted a similar approach, the so-called *hoop*-model: the entanglements localize certain short segments of a particular strand to a small volume.[7] One can model this effect by describing a network strand as a free Gaussian random walk, which is, however, forced to pass through a certain number of hoops, which are fixed in space. Despite a number of differences in the physical models, we shall find that our first model in "Free energy of deformations" leads to similar results.

In addition to the mentioned above, one can find a variety of other theoretical models, some of which are discussed in the review articles.[8–10] More recently, a *slip-tube* molecular model for nonlinear elasticity of entangled polymer networks was introduced.[11] This model combines and generalizes several successful ideas introduced over the years, including Edwards' tube model and the constrained junction model.[12,13] The topological constraints imposed by the neighboring network chains on a given chain are represented by the confining potential that changes upon network deformation.

All theoretical models, describing the macroscopic equilibrium elastic response of densely entangled rubbery networks, have a common purpose—to develop a physically consistent description depicting what one accepts as a correct coarse-grained molecular behavior—but also accounting for a number of experimental results showing substantial deviations in stress–strain response from the ideal phantom-network result $\sigma = \tilde{\mu}(\lambda - 1/\lambda^2)$.[14]

In our current work, we develop a consistent implementation of the classical tube model to take into account the entanglement effects in crosslinked polymer networks within the same framework as in the polymer melt dynamics. We shall present two very different models that both implement ideas from the reptation tube model, but then follow quite different routes. We particularly focus on the entropy of internal reptation motion and resulting re-distribution of chain segments along the tube in a deformed state. The reptation tube model of entangled network strands provides a more accurate description in the sense that it keeps track of the allocation of chain segment excursions in the tubes. In this way, our first model, based on a free energy calculation, closes an important gap among the existing models with some unexpected consequences. The calculations, however, reveal that our results in the limit of high entanglement density are very similar to the ones of the HB model, which approaches network constraints in a different way.

In "Constrained rouse dynamics at $t \to \infty$" we outline our second approach, where we extend our earlier model of constrained Rouse dynamics in viscoelastic networks,[15] to include entanglement constraints. Although the constrained Rouse model was designed as a framework for predicting the dynamic response of a rubbery network, it provides interesting results in the equilibrium time limit. The mechanical behavior of real networks nearly always depart from affine and phantom predictions in two ways: in the shape of the stress–strain relationship and the modulus magnitude. Our second, dynamical model predicts a much larger equilibrium modulus than other molecular models, and also provides a novel way of investigating rubber elasticity in the highly entangled regime.

The article is organized as follows. After briefly reviewing the basic principles of network theory for the case of an ideal phantom network in the following section, "Reptation theory of rubber elasticity" introduces the network tube model and its properties in some detail, and outlines the derivation of the full expression for rubber-elastic free energy. "Free energy of deformation" explores the properties of the full expression for the constrained entropic free energy, examining different limiting cases, as well as its linear-response limit. "Constrained rouse dynamics at $t \to \infty$" presents the second version of the tube model: we construct a microscopic dynamic stress tensor, in a way to include tube constraints as well as network crosslinks. Within this dynamics theory, we solve the stress tensor for a highly entangled polymer in the long-time limit. We conclude by comparing the concepts and the results of this work with previous theories.

CLASSICAL PHANTOM CHAIN NETWORK

Before considering densely entangled rubber, we briefly review the well-known results of the phantom chain network theory, which provides the basic building blocks for most other theoretical models. One way of representing an ideal macromolecule is via the standard Gaussian or *bead-spring* model Figure 1. For the standard Gaussian model, the chain conformation is specified by the set $S = \{\boldsymbol{r}_0, \boldsymbol{r}_1, \ldots, \boldsymbol{r}_N\}$ of N *beads*, which can be thought of as N repeating monomer units of the chain.[2] The conformations of an ideal macromolecule coincide with the random walk path of a Brownian particle. Since Brownian motion is a Markovian process, the ideal chain also belongs to the class of Markov chains. Let $\psi(\boldsymbol{r}_n, \boldsymbol{r}_{n-1})$ represent the linear memory that describes the bonds between a pair of link neighbors. The memory of the chain direction is lost over a distance comparable to its persistence length ℓ. The persistence length of a long, flexible, ideal chain is related to the effective Kuhn segment length of a freely jointed chain of $N = L/\ell$ segments, such that $\langle \boldsymbol{R}^2 \rangle = N\ell^2$. In the context of the Gaussian chain model, the Kuhn step length is defined by $\langle (\boldsymbol{r}_n - \boldsymbol{r}_{n-1})^2 \rangle = \ell^2$, and denoted by the term (RMS) *link length*. The probability of a given polymer shape S is thus given by $\Psi[S] = \prod_{n=1}^{N} \psi(\boldsymbol{r}_n, \boldsymbol{r}_{n-1})$,

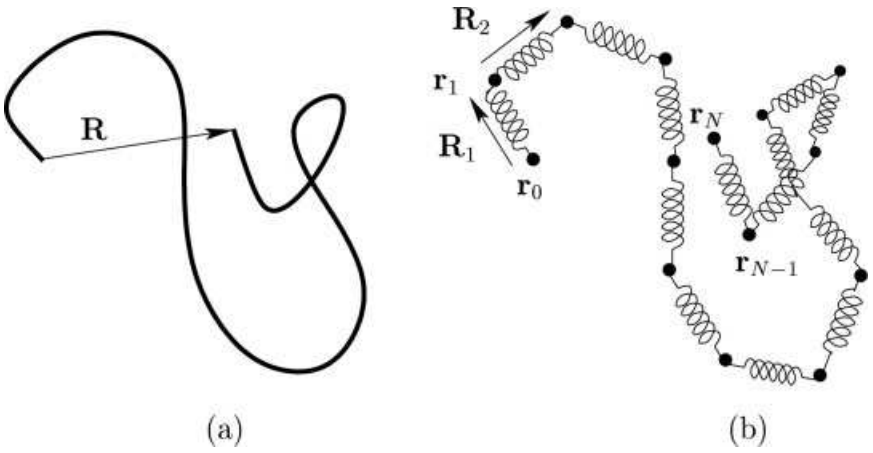

Figure 1. (a) An ideal, long flexible phantom chain, and (b) its Gaussian model counterpart. The shape of the polymer can be represented by the set of position vectors of the beads $S = \{\boldsymbol{r}_0, \boldsymbol{r}_1, \ldots, \boldsymbol{r}_N\}$, or by the set of bond vectors $\{\boldsymbol{R}_1, \boldsymbol{R}_2, \ldots, \boldsymbol{R}_N\}$, where $\boldsymbol{R}_n = \boldsymbol{r}_n - \boldsymbol{r}_{n-1}$. The end-to-end vector $\boldsymbol{R} = \boldsymbol{r}_N - \boldsymbol{r}_0$ characterizes the size of the chain.

and represents the connectivity of the ideal macromolecule. For the bead-spring model, the bond lengths have the Gaussian distribution, such that $\psi(\boldsymbol{r}_n, \boldsymbol{r}_{n-1})$ is defined as follows:

$$\psi(\boldsymbol{r}_n, \boldsymbol{r}_{n-1}) = \left(\frac{3}{2\pi\ell^2}\right)^{3/2} \exp\left\{-\frac{3}{2\ell^2}(\boldsymbol{r}_n - \boldsymbol{r}_{n-1})^2\right\}. \tag{1}$$

The partition function is computed by integrating the distribution $\Psi[S]$ over all possible conformations.[8] When the chain is very long, the monomer index n may be regarded as a continuous variable. In this continuous representation, the discrete bond vector $\boldsymbol{R}_n = \boldsymbol{r}_n - \boldsymbol{r}_{n-1}$ is replaced by the functional derivative $\partial\boldsymbol{r}_n/\partial n$.[2] If the endpoints of the macromolecule are fixed, at say positions $\boldsymbol{r}$ and $\boldsymbol{r}'$ in space, the partition function is the Wiener path integral

$$\mathbb{P}(\boldsymbol{r}, \boldsymbol{r}', N) = \mathcal{N} \int_{\boldsymbol{r}(0)=\boldsymbol{r}'}^{\boldsymbol{r}(N)=\boldsymbol{r}} [\mathcal{D}\boldsymbol{r}] \times \exp\left\{-\frac{3}{2\ell^2}\int_0^N \left(\frac{\partial\boldsymbol{r}_n}{\partial n}\right)^2 dn\right\}, \tag{2}$$

which is a Green's function and a solution of the following diffusion type equation:

$$\left[\frac{\partial}{\partial N} - \frac{\ell^2}{6}\frac{\partial^2}{\partial\boldsymbol{r}^2}\right]\mathbb{P}(\boldsymbol{r}, \boldsymbol{r}'; N) = \delta(\boldsymbol{r} - \boldsymbol{r}')\delta(N). \tag{3}$$

The solution is the Gaussian distribution and gives the number of configurations of a chain with N segments and span $\boldsymbol{r} - \boldsymbol{r}' = \boldsymbol{R}_0$:

$$\mathbb{P}(\boldsymbol{R}_0) = \left(\frac{3}{2\pi\ell^2 N}\right)^{3/2} \exp\left(-\frac{3}{2\ell^2}\frac{\boldsymbol{R}_0^2}{N}\right), \tag{4}$$

which is proportional to the partition function $Z(\boldsymbol{R}_0) = e^{-F(\boldsymbol{R}_0)/k_\mathrm{B}T}$. Each configuration or shape of the chain has the same internal energy associated with bond contortions. Furthermore, the entropic free energy $F(\boldsymbol{R})$ of the given chain is then

$$F(\boldsymbol{R}) = -k_\mathrm{B}T \ln \mathcal{Z}(R) = k_\mathrm{B}T\frac{3\boldsymbol{R}^2}{2N\ell^2} + C, \tag{5}$$

where C is a constant. This result goes back far in history: one can review its derivation and consequences in seminal texts on this subject.[2,16,17]

Consider an ideal network of n elastically active network strands at temperature T, occupying a volume V_i. At network formation, i.e. at crosslinking, each chain in the polymer melt obeys the distribution eq 4, which is then permanently frozen in the network topology. Let each network strand connecting a pair of crosslinks consist of N bonds or segments. Next, consider a homogeneous deformation of the network sample (subscripts i and f will denote *initial* and *final* values, e.g., the initial unstrained area is A_i and a deformed span vector is $\boldsymbol{R}_\mathrm{f}$; the Greek alphabet is used to label the Cartesian coordinate indices), described by macroscopic extension ratio tensor $\boldsymbol{E}$. From the affine deformation approximation, that is, if a macroscopic rubber sample is deformed by $\boldsymbol{E}$, then the end-to-end vector of any subchain between two crosslinks will be equal to $\boldsymbol{R} = \boldsymbol{E}\cdot\boldsymbol{R}_0$, after deformation. Then, from eq 5, the free energy of a given strand after deformation is

$$F(\boldsymbol{R}) = \frac{3\,k_\mathrm{B}T}{2N\ell^2}\boldsymbol{R}_0\cdot\boldsymbol{E}^\top\cdot\boldsymbol{E}\cdot\boldsymbol{R}_0, \tag{6}$$

where we have dropped constants, arising from normalization, independent of the strain $\boldsymbol{E}$. To obtain the free energy $\mathcal{F}$ of the network, one has to sum over the free energy contributions F of all the network strands. *What is the probability that a given network strand has span* $\boldsymbol{R}$*?* We can imagine that the chains, constituting a given, random link, were just touching prior to the permanent linking. The probability of the disorder is then given by the same weight $\mathbb{P}(\boldsymbol{R}_0)$ [see eq 4] as that of thermal equilibrium of the melt prior to an instantaneous network formation. The free energy of the network is thus the average over the distribution $\mathbb{P}(\boldsymbol{R}_0)$ multiplied by the average number n of elastically active network strands in the sample:

$$\mathcal{F}(\boldsymbol{E}) = n\frac{3\,k_\mathrm{B}T}{2N\ell^2}\langle\boldsymbol{R}_\mathrm{i}\cdot\boldsymbol{E}^\top\cdot\boldsymbol{E}\cdot\boldsymbol{R}_\mathrm{i}\rangle_{\mathbb{P}(\boldsymbol{R}_\mathrm{i})} \tag{7}$$

$$= \frac{1}{2}nk_\mathrm{B}T\,\mathrm{Tr}[\boldsymbol{E}^\top\cdot\boldsymbol{E}], \tag{8}$$

where the subscript i refers to the initial condition.

For the specific case of a stretch, such that only the diagonal deformation components $E_{\alpha\alpha} \equiv \lambda_\alpha$ for $\alpha \in \{x, y, z\}$ are nonzero, the deformation free energy eq 8 becomes

$$\mathcal{F}(\boldsymbol{R}) = \frac{1}{2}nk_\mathrm{B}T(\lambda^2 + 2/\lambda) \quad \text{if } \lambda_z = \lambda;\ \lambda_x = \lambda_y = \lambda^{-1/2}, \tag{9}$$

when $\boldsymbol{E}$ is a uniaxial, isovolumetric deformation.

The force required to change the length of the network sample in the z-dimension from L_{z_i} to L_{z_f} is equal to the change in the deformation free

energy eq 9 with respect to change in sample size along the axis of deformation:

$$f_z = \frac{\partial \mathcal{F}}{\partial L_z} = \frac{\partial \mathcal{F}}{\partial(\lambda_z L_{z_i})} = \frac{1}{L_{z_i}} \frac{\partial \mathcal{F}}{\partial \lambda} \tag{10}$$

$$= \frac{nk_B T}{L_{z_i}} \left(\lambda - \frac{1}{\lambda^2}\right). \tag{11}$$

The *true* stress $\sigma_{\alpha\beta}$ in an elastic substance is defined as the ratio between the force applied in the α direction and the cross-sectional area of the strained sample perpendicular to the β-axis. For the current example of uniaxial deformation the true stress is

$$\sigma_{zz} = \frac{f_z}{L_{x_f} L_{y_f}} = \frac{\lambda}{V_i} \frac{\partial \mathcal{F}}{\partial \lambda} \tag{12}$$

$$= \tilde{c} k_B T \left(\lambda^2 - \frac{1}{\lambda}\right), \tag{13}$$

where $\tilde{c} = n/V$ is the average crosslink-density of the network sample. The quantity $\tilde{\mu} = \tilde{c} k_B T$ is the classical rubber modulus responsible for the shear deformations, with magnitude that ranges between 10^4 (for a weak rubber) and 10^6 Pa. A more convenient stress to measure in experiments is the so-called *engineering* or nominal stress defined as the force applied, divided by the *original* unstrained area:

$$\sigma_{zz(\mathrm{eng})} = \frac{f_z}{L_{x_i} L_{y_i}} = \tilde{\mu} \left(\lambda - \frac{1}{\lambda^2}\right). \tag{14}$$

It is customary to draw the stress–strain curves in the Mooney-Rivlin representation, which plots the reduced stress function $f^* \equiv \sigma_{\mathrm{eng}}/(\lambda - 1/\lambda^2)$ against $1/\lambda$. This representation therefore indicates the degree of deviation from the simple phantom chain network behavior, in which $f^* = \mathrm{const}$.

A few positive remarks should be made in defence of this simple model. First, consider the assumption of an end-linking polymer. Since the positions of end points of a single chain fluctuate strongly, the junctions reduce these fluctuations and therefore alter the single chain statistics. However, in spite of an apparent complexity, this effect merely introduces a multiplicative factor of the form $1 - 2/\phi$, where ϕ is the junction point functionality.[18] Second, one can assume that the deformation preserves the volume (implied by the constraint $\det \boldsymbol{E} = 1$), since the bulk (compression) modulus is by a factor of at least 10^4 greater than the rubber modulus $\tilde{\mu}$, a characteristic scale of rubber elastic energies. Incompressibility will be a subject of special discussion later in "Volume relaxation". Third, the quenched average in eq 7 does not average over chains of different arc lengths, but the fact that the result is independent of arc length generalizes the result to apply for chains of arbitrary length, or even for a polydisperse ensemble of chains.

REPTATION THEORY OF RUBBER ELASTICITY

Including topological interactions into a free energy model has remained very difficult. However, it has been shown that a highly entangled polymer network can be treated by a *tube* model. This effective model assumes that the motion of a chain is essentially confined in a tube-like region made of the surrounding polymers. Although the notion of a tube was originally devised for rubbers,[19] it later turned out to be far more successful in explaining dynamical properties of melts.[2]

In this work we follow the original ideas of Edwards: we assume that each network strand is limited in its lateral fluctuations by the presence of neighboring chains.[4] Therefore, each segment of a polymer only explores configurations in a limited volume, which is much smaller than the space occupied by a *phantom* chain. One can imagine the whole strand to fluctuate around a certain trajectory, a mean path, which is called the primitive path in the reptation theory.[4] The most intuitive way to visualize such a trajectory is to imagine that the chain is made shorter and thus stretched between the fixed crosslinking points. The taut portions of the chain will form the broken line of straight segments between the points of entanglement, which restrict the further tightening. This primitive path can be considered as a random walk with an associated typical step length, which is much bigger than the polymer step length, as sketched in Figure 2. The number of corresponding tube segments M is determined by the average number of entanglements per chain (the situation with no entanglements corresponds to $M = 1$).

Effectively, the real polymer is confined by the neighboring chains to exercise its thermal motion only within a tube around the primitive path. Note that all the chains are in constant thermal motion, altering the local constraints they impose on each other. Hence, the fixed tube is a gross simplification of the real situation. However, one expects this to be an even better approximation in rubber than in a corresponding melt (where the

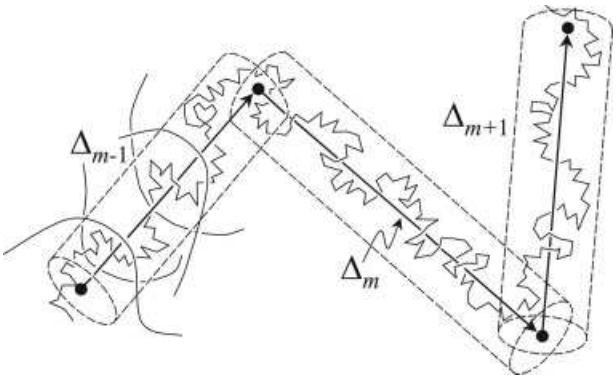

Figure 2. A polymer strand is surrounded by neighboring chains, which effectively confine the strand to a tube. The tube segment m, with the span vector $\mathbf{\Delta}_m$ along its axis, contains s_m monomer steps, where m runs from 1 to M.

success of reptation theory is undeniable), because the restriction on chain reptation diffusion in a crosslinked network eliminates the possibility of constraint release.

To handle the tube constraint mathematically, we traditionally assume that the chain segments are subjected to a quadratic potential, restricting their motion transversely to the primitive path. Along one polymer strand consisting of N monomer segments of effective step length ℓ, there are M tube segments, each containing $s_m, m = 1, \ldots, M$ monomer steps. Since the strand is permanently crosslinked, we infer the obvious condition

$$\sum_{m=1}^{M} s_m = N. \tag{15}$$

In effect, one has two random walks: the topologically fixed primitive path and the polymer chain restricted to move around it—both having the same end-to-end vector $\boldsymbol{R}_0$, between the connected crosslinking points.

Each tube segment m can be described by the span vector $\mathbf{\Delta}_m$, joining the equilibrium positions of the strand monomers at the two ends of each tube segment. The number of tube segments M (or, equivalently, the nodes of the primitive path) is a free parameter of the theory, ultimately determined by the length of each polymer strand and the entanglement density.

Since the primitive path is a topologically frozen characteristic of each network strand, we shall assume that all primitive path spans $\mathbf{\Delta}_m$ deform affinely with the macroscopic strain: $\mathbf{\Delta}'_m = \boldsymbol{E} \cdot \mathbf{\Delta}_m$. This is the central point in the model: the rubber elastic response will arise becasue of the change in the number of polymer configurations in a distorted primitive path. At this stage, one, of course, must assume that there is no constraint release,[20] unlike in the analogous melt or semidilute solution—chain reptation can only proceed confined between the crosslinks. To evaluate the number of conformations, we look separately at chain excursions parallel and perpendicular to the tube axis, along each span $\mathbf{\Delta}_m$. Effectively, this amounts to introducing a new coordinate system for each tube segment, with one preferred axis along $\mathbf{\Delta}_m$. In this direction one recovers the behavior of a free random walk, giving rise to a one-dimensional Gaussian statistics in the long chain limit. Note that only one third of the steps s_m in this tube segment would be involved in such parallel (longitudinal) excursions. We therefore obtain for the number of parallel excursions in a tube segment m:

$$W_m^{\parallel} \propto \frac{1}{\sqrt{s_m/3}} \exp\left[-\frac{\mathbf{\Delta}_m^2}{2\ell^2(s_m/3)}\right]. \tag{16}$$

To determine the number of perpendicular (transverse) excursions, one can introduce the Green's function for the perpendicular steps made by the chain. In effect, we consider a two-dimensional random walk, with a total number of steps $(2s_m/3)$, in a centrosymmetric quadratic potential. For each of these two perpendicular coordinates, the Green's function satisfies the following modified diffusion equation:

$$\left(\frac{\partial}{\partial s} - \frac{\ell^2}{2}\frac{\partial^2}{\partial x_f^2} + \frac{q_0^2}{2}x_f^2\right) G(x_i, x_f; s) = \delta(x_f - x_i)\delta(s), \tag{17}$$

where the x_i and x_f are the initial and final coordinates of the random walk with respect to the tube axis and q_0 determines the strength of the confining potential.[21] This is an essential parameter of many reptation theories, directly related to the tube diameter D. Many discussions can be found in the literature regarding, for instance, the possible dependence of D on entanglement density and the possible change in D on deformation. However, we shall find that the potential strength q_0 does not enter the final elastic energy of a highly entangled rubber, in an approximation that we expect to hold for a majority of cases. Such a universality resembles the situation with phantom networks, where most microscopic chain parameters do not contribute to the final results.

The exact solution of eq 17 is known and is often encountered in the physics of polymers. However, we only need to consider a particular limit $q_0 \ell s_m \gg 1$ of this solution, which is the case of dense entanglements (resulting in a strong confining potential) and/or of a large number s_m of monomers confined in the tube segment. Outside this limit, that is, when the tube diameter is the same order as the contour length of the confined chain, the whole concept of chain entanglements becomes irrelevant. In the case of our present interest, that is, in the strongly confined limit, the solution has a particularly simple form, see ref. 4,

$$G_m(x_\mathrm{i}, x_\mathrm{f}; s_m) \propto \exp\left[-\frac{q_0}{2\ell}\left(x_\mathrm{i}^2 + x_\mathrm{f}^2\right) - \frac{1}{6} q_0 \ell s_m\right]. \tag{18}$$

Remembering that there are two coordinates describing the transverse excursions, we obtain for the two-dimensional Green's function of the tube segment m:

$$G_m(\boldsymbol{r}_\mathrm{i}, \boldsymbol{r}_\mathrm{f}; s_m) \propto e^{-\frac{1}{3} q_0 \ell s_m}\, e^{-\frac{q_0}{2\ell}\left(\boldsymbol{r}_\mathrm{i}^2 + \boldsymbol{r}_\mathrm{f}^2\right)}, \tag{19}$$

where $\boldsymbol{r}_i$ and $\boldsymbol{r}_f$ are the initial and final transverse two-dimensional coordinates. The total number of transverse excursions is proportional to the integrated Green's function:

$$W_m^{\perp} \propto \int d\boldsymbol{r}_\mathrm{i} \int d\boldsymbol{r}_\mathrm{f}\, G_\mathrm{m}(\boldsymbol{r}_\mathrm{i}, \boldsymbol{r}_\mathrm{f}; s_\mathrm{m}) = \mathrm{const} \cdot e^{-\frac{1}{3} q_0 \ell s_m}. \tag{20}$$

Since the Green's function in the approximation eq 19 does not couple the initial or final coordinates to the number of segments s_m, this integration will only produce a constant normalization factor, which can be discarded.

The product of the statistical weights of parallel and perpendicular excursions gives the total number of configurations of a polymer segment consisting of s_m monomers in a tube segment of span $\boldsymbol{\Delta}_\mathrm{m}$:

$$\mathbb{W}_\mathrm{m} = W_m^{\parallel} W_m^{\perp} \propto \frac{1}{\sqrt{s_\mathrm{m}}} \exp\left(-\frac{3}{2\ell^2 s_\mathrm{m}} \boldsymbol{\Delta}_\mathrm{m}^2 - \frac{1}{3} q_0 \ell s_\mathrm{m}\right). \tag{21}$$

Therefore, we find for the full number of configurations of the whole strand by summing over all M steps of the primitive path and integrating over the remaining degrees of freedom, the number of polymer segments confined between each node of the tube:

$$\mathbb{W} = \int_0^N ds_1 \cdots \int_0^N ds_\mathrm{M} \left(\prod_{m=1}^{M} \mathbb{W}_\mathrm{m}\right) \delta\left(\sum_{m=1}^{M} s_\mathrm{m} - N\right), \tag{22}$$

where the constraint eq 15 on the polymer contour length between two crosslinks is implemented by the delta-function. The statistical summation in eq 22 takes into account the reptation motion of the polymer between its two crosslinked ends, by which the number of segments, s_m, constrained within each tube segment can be changed and, thus, equilibrates for a given conformation of primitive path.

Rewriting the delta-function as $\delta(x) = \frac{1}{2\pi} \int dk\, e^{\mathrm{i}kx}$, we proceed by finding the saddle points s_m^*, which make the exponent of the statistical sum eq 22 stationary. It can be verified that the normalization factors $1/\sqrt{s_m}$ contribute only as a small correction to the saddle points

$$s_m^* \approx \left[\frac{3\boldsymbol{\Delta}_m^2}{2\ell^2\left(\frac{1}{3} q_0 \ell + \mathrm{i}k\right)}\right]^{1/2}. \tag{23}$$

The integral in eq 22 is consequently approximated by the steepest descent method. We repeat the same procedure for the integration of the auxiliary variable k, responsible for the conservation of the polymer arc length. The saddle point value k^*, inserted back into eq 23, gives the equilibrium number of polymer segments confined within a tube segment with the span vector $\boldsymbol{\Delta}_m$:

$$s_\mathrm{m} = \frac{N\Delta_m}{\sum_{m=1}^{M} \Delta_m}, \tag{24}$$

where $\Delta_m = |\boldsymbol{\Delta}_m|$ is the length of the m-th step of the primitive path. We finally obtain the total number of configurations of one strand, confined within a tube whose primitive path is described by the set of vectors $\{\boldsymbol{\Delta}_m\}$. The statistical weight $\mathbb{W}$ associated with this state is proportional to the probability distribution:

$$\mathbb{W}(\boldsymbol{\Delta}_1, \ldots, \boldsymbol{\Delta}_M) \propto \mathbb{P}(\{\boldsymbol{\Delta}_m\}) \times \propto e^{-\frac{1}{3} q_0 \ell N} \frac{\exp\left[-\frac{3}{2\ell^2 N}\left(\sum_{m=1}^{M} \Delta_m\right)^2\right]}{\left(\sum_{m=1}^{M} \Delta_m\right)^{M-1}}. \tag{25}$$

This expression is a result analogous to the ideal Gaussian probability $\mathbb{P}_0(\boldsymbol{R}_0)$ in eq 4 for

a nonentangled phantom chain. Note that the chain end-to-end distance $\boldsymbol{R}_0$ is also the end-to-end distance of the primitive path random walk of variable-length steps: $\sum_{m=1}^{M} \boldsymbol{\Delta}_m = \boldsymbol{R}_0$. The probability distribution $\mathbb{P}(\{\boldsymbol{\Delta}_m\})$ for a chain confined in a reptation tube is reminiscent of a normal Gaussian, but is in fact significantly different in the form of the exponent and the denominator.

From eq 25 we obtain the formal expression for free energy, $k_\mathrm{B}T \ln \mathbb{W}$:

$$\frac{1}{k_\mathrm{B}T}F = \frac{3}{2\ell^2 N}\left(\sum_{m=1}^{M}\Delta_m\right)^2 + (M-1)\ln\left(\sum_{m=1}^{M}\Delta_m\right), \tag{26}$$

of a chain confined to a tube with the primitive path conformation $\{\boldsymbol{\Delta}_m\}$, which implicitly depends on the end-to-end vector $\boldsymbol{R}_0$.

FREE ENERGY OF DEFORMATIONS

Next we perform a procedure that is analogous to the one used to obtain eq 7. In the polymer melt before crosslinking, the ensemble of chains obeys the distribution in eq 25, giving the free energy per strand eq 26. The process of crosslinking not only quenches the end points of each of the crosslinked strands, but also quenches the nodes of the primitive path $\boldsymbol{\Delta}_m$, since the crosslinked chains cannot disentangle because of the fixed network topology. In our mean field approach, the tube segments described by $\boldsymbol{\Delta}_m$ are conserved, although they may be deformed by the strains applied to the network. For evaluating the quenched average, note that the statistical weight eq 25 treats the tube segments m in a symmetric way. This allows one to perform the explicit summation over the index m:

$$\begin{aligned}\mathcal{F}/k_\mathrm{B}T &= \left\langle \frac{3}{2\ell^2 N}\left(\sum_{m=1}^{M}\Delta_m\right)^2 + (M-1)\ln\left(\sum_{m=1}^{M}\Delta_m\right)\right\rangle \\ &= \frac{3}{2\ell^2 N}\left(M\langle\Delta_m^2\rangle + M(M-1)\langle\Delta_m\Delta_n\rangle\right) \\ &\quad + (M-1)\left\langle\ln\left(\sum_{m=1}^{M}\Delta_m\right)\right\rangle, \end{aligned} \tag{27}$$

where, in the second term, m and $n \neq m$ are arbitrary indices of the primitive path steps. The brackets $\langle\cdots\rangle$ refer to the average with respect to the weight $\mathbb{P}(\{\boldsymbol{\Delta}_m\})$ given in eq 25.

Furthermore, note that any affine deformation $\boldsymbol{E}$ transforms the vectors $\boldsymbol{\Delta}_m$ into $\boldsymbol{\Delta}'_m = \boldsymbol{E}\cdot\boldsymbol{\Delta}_m$ and, hence, their lengths $\Delta_m = |\boldsymbol{\Delta}_m|$ into $\Delta'_m = |\boldsymbol{E}\cdot\boldsymbol{\Delta}_m|$, but leaves the quenched distribution $\mathbb{P}(\{\boldsymbol{\Delta}_m\})$ unchanged. Keeping this in mind, we can evaluate the averages eq 27, leading to the free energy per chain of the crosslinked network. Appendix A gives a more detailed account of how one evaluates the averages, bearing in mind that the calculation requires integrating an expression eq 25 dependent on the *modulus* of the tube segment vector $\boldsymbol{\Delta}_m$. The resulting average elastic energy density also incorporates the density of crosslinked chains in the system in the ideal rubber modulus $\tilde{\mu} = \tilde{c}k_\mathrm{B}T$:

$$\begin{aligned}\mathcal{F}_\mathrm{elast} &= \frac{2}{3}\tilde{\mu}\frac{2M+1}{3M+1}\mathrm{Tr}(\boldsymbol{E}^\mathsf{T}\boldsymbol{E}) \\ &\quad + \frac{3}{2}\tilde{\mu}(M-1)\frac{2M+1}{3M+1}(\overline{|\boldsymbol{E}|})^2 + \tilde{\mu}(M-1)\overline{\ln|\boldsymbol{E}|}, \end{aligned} \tag{28}$$

where the following notations are employed:

$$\overline{|\boldsymbol{E}|} = \frac{1}{4\pi}\int_{|\boldsymbol{e}|=1} d\Omega\,|\boldsymbol{E}\,\boldsymbol{e}| \tag{29}$$

$$\overline{\ln|\boldsymbol{E}|} = \frac{1}{4\pi}\int_{|\boldsymbol{e}|=1} d\Omega\,\ln|\boldsymbol{E}\,\boldsymbol{e}|. \tag{30}$$

The notation $\overline{(\cdots)}$ refers to the angular integration over the orientations of an arbitrary unit vector $\boldsymbol{e}$.

The expressions (eqs 29 and 30) can be calculated explicitly for particular cases of imposed deformation. An example of such evaluation in the case of uniaxial deformation, where $\boldsymbol{E}$ takes a diagonal form with $E^\parallel = \lambda$ and $E^\perp = 1/\sqrt{\lambda}$, is given in the Appendix A. Corresponding formulae, eqs 61 and 62, need to be inserted into eq 28 to give the full rubber-elastic energy density. In the small deformation limit, where $\lambda = 1+\varepsilon$, the free energy expression eq 28 immediately leads to the Young's modulus Y in $\mathcal{F}_\mathrm{ext} \approx \frac{1}{2}Y\varepsilon^2$ after noting that

$$\begin{aligned}\mathrm{Tr}(\boldsymbol{E}^\mathsf{T}\boldsymbol{E}) &\approx 3 + 3\,\varepsilon^2 \\ \overline{|\boldsymbol{E}|} &\approx 1 + \frac{2}{5}\varepsilon^2 \\ \overline{\ln|\boldsymbol{E}|} &\approx \frac{3}{10}\varepsilon^2. \end{aligned}$$

For small simple shear, we can write the matrix $\boldsymbol{E}$ as $\lambda_{ij} = \delta_{ij} + \varepsilon u_i v_j$, where $\boldsymbol{u}$ and $\boldsymbol{v}$ are two orthogonal unit vectors. As expected, the calculation returns the shear modulus G in $\mathcal{F}_\mathrm{shear} \approx \frac{1}{2}G\varepsilon^2$,

which is equal to one third of the Young's modulus Y:

$$G = \frac{1}{3}Y = \tilde{\mu}\left(\frac{4}{3}\cdot\frac{2M+1}{3M+1} + \frac{1}{5}(M-1)\cdot\frac{11M+5}{3M+1}\right). \tag{31}$$

We point out that the expression (28) is very similar to the free energy density obtained by Higgs and Ball,[7] although they start from a completely different set of physical assumptions and mathematical framework. In HB, the entanglements cause the strands to interact with each other only at certain points. This is modeled by forcing the individual strands to pass through a certain number of independent virtual fixed *hoops*. The hoops effectively divide the polymer strand into segments, each performing a three-dimensional phantom random walk. The apparent similarity of the final expression for the rubber-elastic free energy density is a comforting reflection of consistency in underlying physical concepts and the mathematical treatment of both models. The internal similarity of the models arises from the treatment of local chain reptation, equilibrating the distribution of its segments between the nodes of primitive path, before and after the deformation.

From the expression eq 28, we can recover the ordinary free energy of a phantom chain network by taking the case $M = 1$: $\mathcal{F}_{\text{elast}} = \frac{1}{2}\tilde{\mu}\,\text{Tr}(\boldsymbol{E}^{\mathsf{T}}\boldsymbol{E})$. This limit means physically that the polymer strand is placed in one single tube, tightly confined to the axis. Mathematically, a random walk in three dimensions with the total of N steps is equivalent to a random walk in one dimension along a given direction $\boldsymbol{\Delta}$, with $N/3$ steps, while the two perpendicular excursions in a tightly confining potential do not contribute to the entropic elasticity. This fact is the underlying reason why we recover the phantom chain network result by taking $M = 1$ in our model. Of course, in a parallel "hoop model" of HB, the case $M = 1$ simply means that there are no constraints.

On the other hand, as the number of tube segments M becomes very large, we obtain the elastic energy of the form

$$\mathcal{F}_{\text{elast}} = \tilde{\mu}\,M\big((\overline{|\boldsymbol{E}|})^2 + \overline{\ln|\boldsymbol{E}|}\big). \tag{32}$$

There are two ways to arrive at this limit of $M \gg 1$ in a real physical situation: either the polymer melt is very dense, causing a high entanglement density, or the polymer chain is very long. In the latter case, the polymer strand experiences many confining entanglements along its path.

Recall that the $\mathcal{F}_{\text{elast}}$ is the elastic energy density, which relates to the free energy per chain, such as the eq 26, and is proportional to the density of elastic strands in the system: $\mathcal{F}_{\text{elast}} \propto \tilde{\mu} = \tilde{c}k_{\text{B}}T$, where $\tilde{c}$ is the number of crosslinked strands per unit volume. We can assume that in a melt, or a semidilute solution, the chain density is inversely proportional to the volume of an average chain, hence inversely proportional to the chain contour length: $\tilde{c} \propto 1/L$. In the case of phantom network $\mathcal{F}_{\text{elast}} \to 0$ as the chains become infinitely long! This unphysical result reflects the fact that the phantom chain model assumes the entanglement interactions of the chains irrelevant. Clearly, this assumptions breaks down in the long chain limit, where we expect the entanglements to play a crucial role.

This unphysical feature of phantom network model is overcome by our expression eq 32. As the strands become longer, they will experience more entanglements, generating more primitive path nodes and confining tube segments. One can assume that the number of entanglements scales linearly with the strand length $L : M \propto L$, in fact: $M = N/N_e$ with N_e the characteristic entanglement length, essentially the average value of s_m^*. Considering expression eq 32, with $\tilde{c} = (Nv_{\text{monomer}})^{-1}$ (the inverse volume of the chain in a melt), we note that the corresponding elastic free energy $\mathcal{F}_{\text{elast}}$ does not vanish in the limit $L \to \infty$. At $M \gg 1$, the constant plateau modulus becomes $\tilde{\mu}M = k_BT/N_{\text{e}}v_{\text{monomer}}$. As one expects, in an entangled polymer system, there is no real difference between the network and the melt and they both have the same plateau modulus—with the corollary that the entanglement length N_{e} must be much smaller in the permanently crosslinked network.

One should note that in this article we only work with dry polymer melt systems, aiming at understanding basic principles of combined network and tube constraints. However, an extension to swollen gels is possible and quite straightforward; for instance, the key parameter M has been estimated as $M \propto \phi^{-4/3}$, with ϕ the polymer volume fraction.[22,23]

The current model only describes the equilibrium response of a network to deformation. Shortly after applying the deformation, traditionally assumed affine on the level of primitive path segments, the network finds its chains far from the microscopic equilibrium. Each strand then

redistributes its monomers between the deformed tube segments, attributing more monomers to some segments, less to others. This process proceeds via the local reptation, the sliding motion along the primitive path, and would be reflected by a time dependence of the variable s_m. This number of monomers attributed to the tube segment m is changing, after the deformation, between a the initial value s_m^* in the eq 24 and the corresponding saddle-point value at $\Delta'_m = |\boldsymbol{E} \cdot \boldsymbol{\Delta}_m|$. By describing the associated relaxation process, our model can be naturally extended to describe the short-time viscoelastic response of an ideal crosslinked network (with no loops and dangling ends, leading to long relaxation of stress); the characteristic time of such a reptation dynamics is the Rouse time, since the dominant process is the monomer diffusion along the principal path.

CONSTRAINED ROUSE DYNAMICS AT $t \to \infty$

The Rouse model of beads, each connected to its nearest neighbor with Gaussian springs, is a popular starting point in studying polymer dynamics.[2] Now we construct and solve such a dynamical model, but with a number of crucial minor difference: the overall chain diffusion (zero Rouse mode) is suppressed, the chain ends are immobilized as fixed-position boundary conditions, and the additional entanglement constraints are brought in via the span vectors $\{\boldsymbol{\Delta}_m\}$.

When a polymer liquid is sheared, every segment of the polymer chain will experience a certain friction together with random forces. When the polymer segments move through the surrounding solvent it will of course induce a velocity field in the the liquid and this will be felt by all the segments. In the Rouse model, this effect is neglected and the solvent, together with the rest of the environment, is modeled as a viscous background. In dense polymeric melts, in contrast to normal liquids or dilute polymeric solutions, this first order approach is acceptable. In a recent paper[15] we applied the classic Rouse model to a phantom network: hydrodynamic interactions and topological effects were ignored, with the environment only producing friction without affecting the chain conformations. We obtained a constrained Rouse model of rubber viscoelasticity, which incorporated quenched constraints on its end-boundary conditions. Many elements of the constrained Rouse dynamics are understood since the work of Mooney,[24] but the evaluation of an average stress tensor represented a significant challenge even for a phantom model. A necessary improvement of this model would be to include trapped entanglements and excluded volume effects into the stress–tensor approach. Here we shall briefly show how to construct an improved version of the microscopic stress tensor for a network, where each polymer strand is not only constrained at its linked endpoints, but also by an effective tube.

The first step is to solve the dynamics of a single chain, constrained at its two endpoints. If $\boldsymbol{r}_n$ denotes the position of the nth monomer segment and ζ its friction coefficient, the continuum limit Langevin equation for a Gaussian chain may be written as:

$$\zeta \frac{d\boldsymbol{r}_n}{dt} = k \frac{\partial^2 \boldsymbol{r}_n}{\partial n^2} + \mathbf{f}_n, \tag{33}$$

where $k = 3k_B T/\ell$ is a simple harmonic spring constant and $\boldsymbol{f}_n$ the stochastic force (white thermal noise). The motions of different monomer segments are correlated due to chain connectivity, as represented by the elastic force, the quadratic term in eq 33. Dynamics of the whole chain can thus be described by a set of N normal modes.

In a network, the chain ends are permanently crosslinked and thus constrained to a certain extent. We shall assume them to be completely fixed, i.e. $\boldsymbol{r}_{n\to 0} = 0$ and $\boldsymbol{r}_{n\to N} = \boldsymbol{R}$. If satisfy these boundary conditions by decomposing the harmonic oscillator motion of eq 33 into normal modes $\{\boldsymbol{x}_p\}$, as follows:

$$\boldsymbol{r}_n(t) = 2\sum_{p=1}^{\infty} \boldsymbol{x}_p(t) \sin\left[\frac{(p-1/2)\pi\, n}{N}\right], \tag{34}$$

which transforms the Langevin equation to a set of decoupled Rouse equations:

$$\zeta_R \frac{d\mathbf{x}_p}{dt} = -k_p\, \mathbf{x}_p + \hat{\mathbf{f}}_p, \tag{35}$$

with $\langle \hat{f}_{p\alpha}(t) \hat{f}_{q\beta}(t') \rangle = 2\zeta_R k_B T \delta_{pq} \delta_{\alpha\beta} \delta(t-t')$ (where $\zeta_R \equiv 2N\zeta$) and the initial conditions $\mathbf{x}_p(0)$. As usual, this is a diffusion problem for an effective "particle" in a harmonic potential with a constant

$$k_p = \frac{2\pi^2 k (p-1/2)^2}{N} = \frac{6\pi^2 k_B T}{N\ell^2}(p-1/2)^2.$$

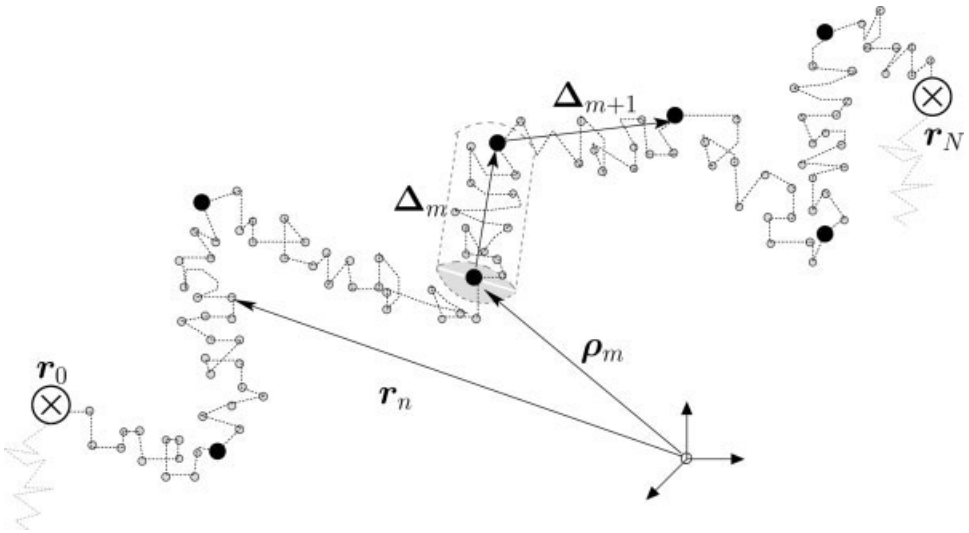

Figure 3. A polymer strand between crosslinks (⊗), confined by M tube segments (only the tube of segment m is explicitly shown here). A tube segment m, with the span vector $\boldsymbol{\Delta}_m = \boldsymbol{\rho}_m - \boldsymbol{\rho}_{m-1}$ along its axis, contains s_m monomer steps. The nth monomer has position vector $\boldsymbol{r}_n$. The end-to-end vector of the polymer strand is $\boldsymbol{R} = \boldsymbol{r}_N - \boldsymbol{r}_0$.

The above formulation is an essential ingredient for studying phantom network dynamics, but is so far only applicable to a single, constrained chain. Next, we consider a random network of such end-linked chains, deformed by strain tensor $\boldsymbol{E}$, and let each strand $\boldsymbol{R}_0$ (between two connected junction points) be deformed affinely, that is, $\boldsymbol{R} = \boldsymbol{E} \cdot \boldsymbol{R}_0$. We assume that the network is initially isotropic. Crosslinks are permanent and will impose the topological constraints on the chains, given that the crosslink density is high enough. If we want to improve on the phantom model by taking into account the neighboring strands, we have to impose another topological constraint.

Following the ideas mentioned in "Reptation theory of rubber elasticity", we imagine each polymer strand to be confined within M tube-like regions. The axis or primitive path of a tube represents all the conformations that are accessible to a chain section, between two entanglement constraints. In Figure 3 we define the current model variables. Let n_m be the polymer segment at tube segment m, so that $n_M = N$, for a chain with N polymer segments between two crosslinks and confined to M tube segments. If s_m is the number of monomer steps within a tube segment labelled m, then $s_m = n_m - n_{m-1}$. The monomer segments have position vectors $\boldsymbol{r}_n(t)$ and the tube segments have position vectors $\boldsymbol{\rho}_m$,

$$\boldsymbol{\rho}_m(t) = 2\sum_{p=1}^{\infty} \boldsymbol{x}_p(t) \sin\left[\frac{(p-\frac{1}{2})\pi\, n_m}{N}\right]. \qquad (36)$$

The microscopic stress tensor $\sigma_{\alpha\beta}$ of a viscoelastic material consists of the stress contribution due to the polymers, the solvent molecules and an isotropic pressure term $\sim k_{\mathrm{B}}T\delta_{\alpha\beta}$.[2] For a rubbery network, the last two contributions play a minor role and is thus neglected from here onwards. For the Rouse model of constrained chains, the stress tensor of a tube segment m, in the continuous limit, is given by

$$\sigma_{\alpha\beta}^{(m)} = \frac{c}{N}\, k \int_{n_{m-1}}^{n_m} dn \left\langle \frac{\partial r_{n\alpha}}{\partial n} \frac{\partial r_{n\beta}}{\partial n} \right\rangle_{\psi}, \qquad (37)$$

where c is the monomer density. The notation $\langle \ldots \rangle_{\psi}$ denotes the time-average of the components of stochastic force $\hat{\mathbf{f}}_p(t)$ over the distribution

$$\psi\left[\hat{f}_{p\alpha}(t)\right] \propto \exp\left(-\frac{1}{4\zeta_{\mathrm{R}}k_{\mathrm{B}}T}\int dt\, \hat{f}_{p\alpha}(t)^2\right). \qquad (38)$$

By summing $\sigma_{\alpha\beta}^{(m)}$ over M tube segments, one defines the microscopic stress tensor for a single chain between crosslinks. The stress tensor of the whole network can be expressed as the ensemble average of $\sigma_{\alpha\beta}^{(m)}$ over the quenched probability to find a given tube-confined strand with tube vectors described by the set $\{\boldsymbol{\Delta}_m\}$. This probability is proportional to the total number of

configurations of the whole crosslinked strand, given by $\mathbb{W}$ in eq 22; its normalization factor will be denoted by $\mathcal{N}_{\mathbb{W}}$, and is computed as follows:

$$\left(\int \prod_{\tilde{m}=1}^{M} d\boldsymbol{\Delta}_{\tilde{m}}\right)\left(\int \prod_{\tilde{m}=1}^{M} ds_{\tilde{m}}\right) \times \prod_{\tilde{m}=1}^{M} e^{-\frac{3\boldsymbol{\Delta}_{\tilde{m}}^2}{2\ell_{\tilde{m}}^2}-\frac{1}{3}q_0\ell s_{\tilde{m}}}\,\delta\left(\sum_{\tilde{m}=1}^{M} s_{\tilde{m}}-N\right). \quad (39)$$

Note that $\boldsymbol{\Delta}'_m = \boldsymbol{E}\cdot\boldsymbol{\Delta}_m$, since $\sum_{m=1}^{M}\boldsymbol{\Delta}_m = \boldsymbol{R}_0$. Crucially, we implement this affine deformation constraint with a delta function to obtain the expression for the network stress tensor, in its most compact form:

$$\sigma_{\alpha\beta}(t) = \tilde{c}\,k\sum_{m=1}^{M}\left[\int_{n_{m-1}}^{n_m} dn\left\langle \dot{\boldsymbol{r}}_\alpha\dot{\boldsymbol{r}}_\beta\,\delta(\boldsymbol{E}\cdot\boldsymbol{\Delta}_m-\boldsymbol{\Delta}'_m)\right\rangle_{\psi}\right]_{\mathbb{W}(\boldsymbol{\Delta}_{\tilde{m}},s_{\tilde{m}})} \quad (40)$$

where $\tilde{c}$ is the crosslink density. It is important to remember that there are two constraints in the average: one on the polymer contour length given by eq 15 and one the tube span vectors.

After rewriting both delta-constraints as their equivalent Fourier integrals, e.g. $\delta(\boldsymbol{E}\cdot\boldsymbol{\Delta}_m-\boldsymbol{\Delta}'_m)\rightarrow d\boldsymbol{\phi}_m\,e^{-i\boldsymbol{\phi}_m(\boldsymbol{E}\cdot\boldsymbol{\Delta}_m-\boldsymbol{\Delta}'_m)}/(2\pi)^3$, we proceed by doing the Gaussian integrations over $\boldsymbol{\Delta}_m$ and the auxiliary vector field $\boldsymbol{\phi}_m$. At this point, the stress tensor becomes

$$\sigma_{\alpha\beta}(t) = \frac{\tilde{c}k\,\mathcal{N}_{\mathbb{W}}^{-1}}{[\det\mathbf{E}\mathbf{E}^{\top}]^{\frac{1}{2}}}\sum_{m=1}^{M}\int\frac{d\phi}{2\pi}e^{i\phi N}\int_0^N ds_1\ldots\int_0^N ds_M e^{-\left(\frac{1}{3}q_0\ell+i\phi\right)\sum_{m'=1}^{M}s_{m'}} \left[\prod_{\tilde{m}=1,\tilde{m}\neq m}^{M}\left(\frac{3}{2\pi s_{\tilde{m}}\ell^2}\right)^{-3/2}\right]\left\langle e^{-\frac{3}{2s_m\ell^2}\boldsymbol{\Delta}_m'^{\top}\cdot(\mathbf{E}\mathbf{E}^{\top})^{-1}\cdot\boldsymbol{\Delta}'_m}\right. \left\{\frac{4\pi}{N}\sum_{p\neq q}x_{p\alpha}x_{q\beta}(p-\tfrac{1}{2})(q-\tfrac{1}{2})\left[\frac{\sin[p-q]\cos[[p-q]]}{p-q}+\frac{\sin[p+q-1]\cos[[p+q-1]]}{p+q-1}\right] +\frac{2\pi^2}{N^2}\sum_p x_{p\alpha}x_{p\beta}\left(p-\tfrac{1}{2}\right)^2\left[s_m+\frac{N\sin[p-\frac{1}{2}]\cos[[p-\frac{1}{2}]]}{\pi\left(p-\frac{1}{2}\right)}\right]\right\}\left.\right\rangle_{\psi[f]}, \quad (41)$$

where the following square bracket notation is used throughout:

$$\sin[\mathsf{x}]\equiv\sin\left[\frac{\pi\mathsf{x}s_m}{2N}\right] \quad ; \quad \times\cos[[\mathsf{x}]]\equiv\cos\left[\frac{\pi\mathsf{x}(n_m+n_{m-1})}{2N}\right]. \quad (42)$$

The deformed tube vector $\boldsymbol{\Delta}'_m$ above can easily be written in terms of normal coordinates $\{\boldsymbol{x}_p\}$, as in eq 36,

$$\boldsymbol{\Delta}'_m = \boldsymbol{\rho}_m-\boldsymbol{\rho}_{m-1} \quad (43)$$

$$= 4\sum_p \boldsymbol{x}_p(t)\sin\left[p-\tfrac{1}{2}\right]\cos[[p-\tfrac{1}{2}]]. \quad (44)$$

The same is done for the term $\int dn\langle\dot{\boldsymbol{r}}_\alpha\dot{\boldsymbol{r}}_\beta\rangle$ in eq 40 and produces the last two lines within the curly brackets in eq 41. At this point, the stress expression in eq 41 depends on the solution of the Langevin equation eq 35 (and thus time), the specific type of deformation $\boldsymbol{E}$ as well as the number of monomers s_m confined in a tube m. We have effectively swapped the order of evaluating the averages, when compared with Reptation theory of rubber elasticity.

To investigate the entire time-spectrum of the linear response, we now need to use the full solution of the Langevin equation (35) describing the normal modes, and depending explicitly on the initial condition of the normal modes:

$$x_{p\alpha}(t) = x_{p\alpha}(0^+)\,e^{-t/\tau_p}+\frac{1}{\zeta_{\mathrm{R}}}\int_0^t e^{-(t-t')/\tau_p}\,\hat{f}_{p\alpha}(t')\,dt' \quad (45)$$

where $\tau_p \equiv \zeta_R/k_p$ is the mode relaxation time. This defines the famous Rouse time, the longest time of relaxation of the lowest ($p = 1$) collective mode of a chain N-segments long: $\tau_R = \zeta N^2\ell^2/(3\pi^2 k_B T)$. In equilibrium, the time-correlation functions of $x_{p\alpha}(0)$ are given by,

$$\langle x_{p\alpha}(t)x_{q\alpha}(0)\rangle_{\psi[f]} = \delta_{pq}\delta_{\alpha\beta}\frac{k_B T}{k_p}e^{-t/\tau_p}, \qquad (46)$$

where $\tau_p = \zeta_R/k_p \equiv \tau_R/(p-1/2)^2$ is the relaxation time of the pth Rouse mode. At arbitrarily short time after an instantaneous strain, we assume that the positions of *all* the segments between two crosslinks are changed in the same proportion as the macroscopic strain $\boldsymbol{E}$ dictates. Thus, after applying a step strain $\boldsymbol{E}$ at time $t = 0$, a given segment position before deformation $\boldsymbol{r}_n(0^-)$ will change to $\boldsymbol{r}_n(0^+)$ *after* deformation,

$$\boldsymbol{r}_n(0^+) = \mathbf{E}\cdot\boldsymbol{r}_n(0^-) \longrightarrow \mathbf{x}_p(0^+) = \mathbf{E}\cdot\mathbf{x}_p(0^-). \quad (47)$$

The second equality follows from the fact that the real segment positions $\{\boldsymbol{r}\}$ are linear functions of the normal coordinates eq 34. Applying the affine deformation to all normal modes, the right-hand side of eq 45 becomes

$$E_{\alpha\mu}\,x_{p\mu}(0^-)\,e^{-t/\tau_p} + \frac{1}{\zeta_R}\int_0^t e^{-(t-t')/\tau_p}\,\hat{f}_{p\alpha}(t')dt'. \quad (48)$$

After substituting this $x_{p\alpha}(t)$ into the main expression for stress, eq 41, we obtain an expression with the Gaussian path integrals having quadratic *and* linear cross-terms in the random force $\boldsymbol{f}_p$, shown in eq 66 in Appendix B. After performing the functional integrations with respect to the random noise, one obtains a beast of an expression that depends on several trigonometric functions of s_m and $(n_m + n_{m-1})$ in a complicated way.

At this point, we diverge from the dynamics calculation and make two assumptions. First, we take the $t \to \infty$ limit as we are presently only interested in equilibrium rubber elasticity. Second, we shall work in the highly entangled regime where $M \gg 1$, or equivalently, $s_m/N \ll 1$. The second assumption allows us to expand the stress tensor expression up to quadratic terms in s_m, thus revealing a more tractable expression:

$$\sigma_{\alpha\beta}(\infty) = \frac{\tilde{c}k\,\mathcal{N}_{\mathbb{W}}^{-1}}{[\det\mathbf{E}\mathbf{E}^{\top}]^{\frac{1}{2}}} \times \int\frac{d\phi}{2\pi}e^{i\phi N}\left[\int_0^N ds e^{-\left(\frac{1}{3}q_0\ell+i\phi\right)s}\left(\frac{3}{2\pi s\ell^2}\right)^{-3/2}\right]^{M-1} \times \sum_{m=1}^{M}\int_0^N ds_m\left(\Xi_1 s_m - \Xi_2 s_m^2\right)e^{-\left(\frac{1}{3}q_0\ell+i\phi\right)s_m}, \quad (49)$$

where Ξ_1 and Ξ_2 are factors dependent on $(n_m + n_{m-1}), N$ and the imposed strain $\boldsymbol{E}$:

$$\Xi_1 = \frac{2\ell^2}{3N}\left[\sum_{p\neq q=1}^{N}\cos^2[[p]]\cos^2[[q]] + \sum_{p=1}^{N}\cos^2[[p]](1+\cos[[2p]])\right]$$

$$\Xi_2 = \frac{2\ell^2}{3N^2}\left[\left(2E_{\alpha\alpha}^{-2} + \sum_{i=1}^{3}E_{ii}^{-2}\right)\sum_{p\neq q}\cos^2[[p]]\cos^2[[q]] + 2\sum_{i=1}^{3}E_{ii}^{-2}\sum_{p}\cos^2[[p]](1+\cos[[2p]])\right]. \quad (50)$$

Note that we have chosen a diagonal deformation in the above expression.

There are several ways of performing the integration with respect to s_m. We prefer a steepest descents method, as it gives a more intuitive answer for the most probably value for s_m. In this way we obtain a saddle point value of $s_m^* \approx 1/(q_0\ell/3 + i\phi)$. To deal with the unknown value $n_m - n_{m-1}$, we choose to approximate it with the sum over monomer segments in a tube segment m, which is proportional to s_m^*:

$$n_m + n_{m-1} \approx 2\sum_{i=1}^{m}s_i \sim 2m\,s_m^*. \qquad (51)$$

For long, highly entangled polymer strands, the sums in eq 50 simplify greatly, for example: $\sum_r \cos^2[[r]] \approx N/2$. This is a very simple approach, but a reasonable way of treating an essentially self-consistent and complicated problem.

After integrating the $[\ldots]^{(M-1)}$ term in eq 49, one can perform the last integration with respect to the auxiliary scalar field ϕ. This is also done by means of a steepest descents method and consequently we obtain the expression for the stress

tensor $\sigma_{\alpha\beta}$. To present it in the manageable form, we now specifically focus on the case of diagonal deformation $\boldsymbol{E}$ and take the explicit limit of $t \to \infty$; the corresponding diagonal components of the stress tensor take the form:

$$\sigma_{\alpha\alpha}(\infty) = \frac{3\tilde{c}k_{\mathrm{B}}T}{[\det \mathbf{E}\mathbf{E}^{\top}]^{\frac{1}{2}}} \left\{ \left(\frac{N}{3}+1\right)\left(\frac{M}{N}\right)^{3/2} - \frac{2}{3}\left(\frac{M}{N}\right)^{1/2}\left[N\left(2E_{\alpha\alpha}^{-2} + \sum_{i=1}^{3} E_{ii}^{-2}\right) + 6\sum_{i=1}^{3} E_{ii}^{-2}\right]\right\} \tag{52}$$

(here no summation over repeated indices is assumed, unless written explicitly). Consider this stress expression for the particular case when $\boldsymbol{E}$ is a uniaxial deformation with primary extension ratio λ in the $\hat{z}$-direction, i.e. $E_{zz} = \lambda; E_{xx} = E_{yy} = \lambda^{-1/2}$. In this type of deformation, the side surfaces are stress-free and one would therefore expect the corresponding principal stresses to be 0. However, from eq 52 it is clear that $\sigma_{xx} = \sigma_{yy} \neq 0$. The original constrained Rouse model of viscoelasticity faced the same "puzzle".[15] Most rubber-elasticity theories calculate the *change* in free energy upon deforming the network sample. Before determining the expressions for the stress, any indeterminate pressure terms are by that stage already subtracted or are simply discarded, since they do not depend on the deformation λ. For this reason seminal literature always mentions that it is important to examine *relative* stress expressions only, cf. ref. 25. It is known that these arbitrary pressure terms are due to a change in the volume of the network system during deformation. However, one cannot accept that hydrostatic pressure is different in an open sample with stress-free boundaries. We have to look more carefully at the effect of volume relaxation on these stress expressions. Since the present model works with the stress tensor from the onset—in contrast with a partition function and associated free energy, such as most models—it is important to deal with this phenomenon correctly.

VOLUME RELAXATION

Consider an initial polymer melt sample of volume V_0. After sufficient crosslinking, a network is formed, contained in a volume V, smaller than the initial volume. This volume change, or syneresis, is caused by the reduction in overall entropy due to crosslinking, and is penalized by a bulk energy contribution $\frac{1}{2}\tilde{K}(\det \boldsymbol{E} - 1)^2$ in the elastic-free energy density, and correspondingly in stress by the amount $\tilde{K}(\det \boldsymbol{E} - 1)$. Here, $\tilde{K}$ is a very large bulk modulus usually of the order $10^9 \mathrm{J/m}^3$ or greater.[26]

Our first task is to determine what the impact of syneresis is on the stress tensor expression. Denote by $\boldsymbol{E_0}$, the initial deformation associated with volume relaxation after network formation. Since we expect this deformation to be small relative to any future imposed strain, as well as being isotropic, we have $\boldsymbol{E_0} = (1+a_0)\boldsymbol{I}$. For simplicity, we consider first the case of no additional externally imposed deformation. Then, the stress tensor eq 52 is only a function of a_0:

$$\sigma_{\mathrm{syn},\alpha\beta} = 3\tilde{c}k_{\mathrm{B}}T\left\{A_1(1+a_0)^{-3} - A_0(1+a_0)^{-5}\right\} + \tilde{K}\left[(1+a_0)^{-3} - 1\right],$$
$$\text{with} \quad A_1 = \left(\frac{1}{3}N+1\right)\left(\frac{M}{N}\right)^{3/2} \quad \text{and} \quad A_0 = \frac{2}{3}(5N+18)\left(\frac{M}{N}\right)^{1/2}. \tag{53}$$

After network formation, the system will reach its equilibrium state, which implies that all the resultant stresses should be 0. Since the correction a_0 is expected to be small, we can expand eq 53 up to linear order in a_0 and solve for $\sigma_{\mathrm{syn},\alpha\beta} = 0$. This step is equivalent to minimizing the free energy density of the system as discussed in detail in ref. 26. The equilibrium solution for this syneresis correction is found to be:

$$a_0^* = \frac{-3\tilde{c}k_{\mathrm{B}}T(A_1 - A_0)}{3\tilde{c}k_{\mathrm{B}}T(5A_0 - 3A_1) + 3\tilde{K}} \quad \propto \quad -\frac{\tilde{c}k_{\mathrm{B}}T}{\tilde{K}} \ll 1. \tag{54}$$

Next, imagine imposing an external deformation $\boldsymbol{E}$, for example the uniaxial extension. During this deformation, a second volume relaxation is possible and should also be accounted for. The total deformation therefore takes the form $\boldsymbol{E}_{\mathrm{tot}} = \boldsymbol{E}_{\mathrm{uni}}(1+a)(1+a_0^*)$, where $\boldsymbol{E}_{\mathrm{uni}}$ is the strictly isovolumetric strain tensor and the syneresis a_0^* is given by eq 54. When the sample is strained, it will lead to the well-known rubber elastic response, but *also* to an additional small bulk compression, represented by a, which is dependent on the imposed strain λ. Again, the underlying physical reason for this extra compression is the further reduction in conformational entropy on deformation. Substituting the total deformation into the stress

tensor eq 52, we have for the nonzero diagonal components, e.g. the $\hat{x}$-component:

$$\sigma_{xx} = 3\tilde{c}k_{\mathrm{B}}T\big\{(1-3a_0-3a)A_1 - (1-5a_0-5a)A_2\big\} + 3\tilde{K}(a_0+a),$$
$$\text{where}\quad A_2 = \frac{2}{3}\left(\frac{M}{N}\right)^{1/2}[(N+6)\lambda^{-2}+4\lambda(N+3)]. \tag{55}$$

The required second volume-relaxation correction a is obtained by demanding that for, e.g., uniaxial extension in the $\hat{z}$-direction, we should have $\sigma_{\mathrm{uni},xx} = \sigma_{\mathrm{uni},yy} = 0$. Again, by expanding the stresses up to first order in a, as shown in eq 55, one obtains a^* for which only $\sigma_{\mathrm{uni},zz}$ is nonzero (for the chosen axes and the principal imposed strain λ):

$$a^* = \frac{3\tilde{c}\,k_{\mathrm{B}}T[(3A_1-5A_2)\,a_0^* + A_2 - A_1] - 3a_0^*\,\tilde{K}}{3\tilde{c}\,k_{\mathrm{B}}T(5A_2-3A_1)+3\tilde{K}}, \tag{56}$$

where a_0^* is given in eq 54. On substituting both volume relaxation factors into eq 55, one obtains the zero-stress conditions on free surfaces. To find out what effect these volume corrections have on the nonzero stress component, we rewrite the stress tensor $\sigma_{\alpha\beta}$ in eq 52, for $\alpha=\beta=z$, in terms of the complete deformation $\boldsymbol{E}_{\mathrm{tot}} = \boldsymbol{E}_{\mathrm{uni}}\,(1+a)(1+a_0^*)$:

$$\sigma_{zz} = 3\tilde{c}k_{\mathrm{B}}T\big\{(1+3a_0)^{-3}(1+3a)^{-3}A_1 - (1+5a_0)^{-5}(1+5a)^{-5}A_3\big\} + \tilde{K}[(1+a_0)^3(1+a)^3-1],$$
$$\text{where}\quad A_3 = \frac{2}{3}\left(\frac{M}{N}\right)^{1/2}\left[2\lambda(N+6)+\frac{3}{\lambda^2}(N+2)\right]. \tag{57}$$

Lastly, after substituting a^* to eq 57, we can now take the limit $\tilde{K}\to\infty$ and obtain the correct expressions for the stress in uniaxial deformation:

$$\sigma_{zz} = 4\,\tilde{c}\,k_{\mathrm{B}}TM^{1/2}N^{1/2}\left(\lambda-\frac{1}{\lambda^2}\right)$$
$$\sigma_{xx} = \sigma_{yy} \quad = \quad 0. \tag{58}$$

The stress σ_{zz} vanishes when there is no deformation, that is, when $\lambda = 1$. This behavior is expected, but is only obtained here *after* accounting for the bulk modulus term and by including small corrections to the overall strain tensor $\boldsymbol{E}$ due to volume relaxations. There are alternative approaches used in continuum mechanics of large deformations, e.g. refs. 27 and 28, based on keeping the rigid constraint of Det $\boldsymbol{E} = 1$ by means of a Lagrange multiplier which has the meaning of system pressure (so that the actual stress is $\sigma_{\alpha\beta} - P\delta_{\alpha\beta}$). There are, however, many negative consequences of independently defining the hydrostatic pressure in a solid system with open boundaries.

CONCLUSION

In this article, we have analyzed the elastic behavior of a polymer network in the presence of entanglements, which are treated within a classical mean-field tube model. By evaluating the constrained configurational entropy, we found that this leads to an elastic free energy which is similar to the one derived in the hoop model of HB.[7] We claim that our model captures the physics of entanglements in a better way than HB, since the entanglements at a microscopic level do not so much localize the polymer at fixed points in space along its path, but rather impede the chain fluctuations on a length scale, which is much larger than the size of monomers. This is due to the fact that the entanglements are caused by neighboring strands, which likewise fluctuate. In this sense, our model provides a firmer ground of the theoretically known and experimentally tested results.

Our second model, based on the constrained Rouse dynamics of "Constrained Rouse dynamics at $t\to\infty$", is also in good agreement with basic experimental data. We fulfilled three aims with the stress tensor approach. The first was to extend the basic framework for a consistent model of the dynamic response,[15] to include entanglement constraints. Second, in the equilibrium long-time limit, we obtained the ideal shape for the stress–strain relationship. Last, we obtained a constant plateau modulus that is $\sqrt{MN}$ times larger than $\tilde{\mu}$, the ideal rubber modulus predicted by phantom models, for a rubber with a high degree of entanglement. We can compare our two models presented in this article in the high entanglement regime, that is, for $M \gg 1$. In the small deformation limit, where $\lambda \to 1+\varepsilon$, the free energy of deformation given by eq 32 can be expanded in terms of the small factor ε as follows:

$$\mathcal{F}_{\mathrm{elast}} \approx \frac{1}{2}Y_1\varepsilon^2 \quad \text{with} \quad Y_1 \approx 2\tilde{c}k_{\mathrm{B}}TM \tag{59}$$

where the Young modulus Y_1, the modulus of extension, is three times the shear modulus and

$\tilde{c}$ is the average crosslink density. In the second, dynamic stress model, we computed the stress tensor from the onset, and on expanding the uniaxial deformation result in eq 58 in terms of ε, we find

$$\sigma \approx Y_2\varepsilon \quad \text{with} \quad Y_2 \approx 12\tilde{c}k_BTM^{1/2}N^{1/2}. \qquad (60)$$

The second model seems most promising in predicting the magnitude for the rubber plateau modulus depending on the geometric mean of the number of chain segments and entanglements, especially if we could compare the value to an end-linked system where N is more or less fixed. It also has a perhaps more appropriate concept development, starting from the dynamical relaxation of segments within the primitive path tube, and then carefully taking the solution to the $t \to \infty$ limit. However, since both models predict a modulus dependent on the degree of entanglement M, a parameter difficult to obtain quantitatively, one needs to investigate more detailed model predictions to assess the success of failure of either approach.

One must acknowledge the fact that developing a "new" model of rubber elasticity today, after a number of excellent advances in this field from all directions, may require better justification. One real aim might be to improve or polish the existing theories, enabling them to account for various known deviations from classical response (especially in the area of biaxial deformations). This was not our goal here, and the models we discussed here are only developed on their basic level: many famous details are left out completely, such as the tube dependence on deformation, partial (loop) disentanglement in the network, Our aim has been to explore in greater depth the fundamental statistical–mechanical concepts behind the doubly constrained (crosslinks and tube) polymer statistics, as well as the global macroscopic constraints such as compressibility. To this end, both models of rubber elasticity discussed here are developed to the accurate and self-consistent level, with the second (Rouse dynamics) approach offering a number of new and not yet fully understood conclusions and observations.

We appreciate many valuable discussions with S.F. Edwards and Mark Warner. S.K. and W.L.V. gratefully acknowledge support from an Overseas Research Scholarship, the Cambridge Overseas Trust, Corpus Christi College and the Commonwealth Scholarship, Gonville and Caius College, respectively.

APPENDIX A: EVALUATION OF QUENCHED AVERAGES $\langle \Delta_M \Delta_N \rangle$ AND $\left\langle \mathrm{LN}\left(\sum \Delta_M\right)\right\rangle$

To evaluate the thermodynamic average $\langle \Delta_m \Delta_n \rangle$, $m,n = 1,\ldots,N$ in the general case, one needs to average $\Delta_m\Delta_n = |\boldsymbol{\Delta}_m||\boldsymbol{\Delta}_n|$ with the probability distribution given by eq 25. For this purpose, one first has to find the normalization $\hat{\mathcal{N}}$ of the distribution, which can most easily be achieved by introducing a new scalar variable $u = \sum_{m=1}^{M} \Delta_m$ to simplify the exponent of this distribution:

$$\begin{aligned}
\hat{\mathcal{N}} &= \prod_{m=1}^{M} \int d\boldsymbol{\Delta}_m \frac{\exp\left(-\frac{3}{2b^2N}\left(\sum_{m=1}^{M}\Delta_m\right)^2\right)}{\left(\sum \Delta_m\right)^{M-1}} \\
&= \prod_{m=1}^{M} \int d\boldsymbol{\Delta}_m \int_0^\infty du\, \delta\left(u - \sum_{m=1}^{M}\Delta_m\right) \frac{e^{-\frac{3}{2b^2N}u^2}}{u^{M-1}} \\
&= (4\pi)^M \int_0^\infty du \frac{e^{-\frac{3}{2b^2N}u^2}}{u^{M-1}} \underline{\int_0^u d\Delta_1\Delta_1^2 \int_0^{u-\Delta_1} d\Delta_2\Delta_2^2 \cdots} \\
&\qquad \underline{\int_0^{u-\cdots-\Delta_{M-2}} d\Delta_{M-1}\Delta_{M-1}^2 \cdot (u-\Delta_1-\cdots-\Delta_{M-1})^2}
\end{aligned}$$

In the last step, we introduced spherical coordinates for the variables $\boldsymbol{\Delta}_m$, implemented the constraint $u = \sum \Delta_m$ and used the fact that the variables Δ_m are bound to be positive. The underlined expression is a function of u, which we call $I_M(u)$. Since the integrals only involve power functions, $I_M(u)$ itself is a power in u, whose order can be determined by counting the dimensions:

$$I_M(u) = \frac{1}{X_M} u^{3M-1}.$$

After noting the recursive structure of $I_M(u)$, one can find a recursion relation for the coefficients X_M:

$$X_{M+1} = \frac{1}{2} 3M(3M+1)(3M+2)X_M.$$

Since $I_{M=1}(u) = u^2$, all coefficients X_M and hence all functions $I_M(u)$ are known. The remaining integration of u is a standard Gaussian integral.

Having obtained the normalization constant $\hat{\mathcal{N}}$, we can proceed to calculate the averages $\langle \Delta_m \Delta_n \rangle$. The calculations are very similar to the earlier one for $\hat{\mathcal{N}}$; the only significant difference is the angular part of the integration which produces terms of the form $\frac{1}{3}\mathrm{Tr}(\boldsymbol{E}^{\mathrm{T}}\boldsymbol{E})$ and $|\overline{\boldsymbol{E}}|$ for the case $m = n$ or $m \neq n$ respectively.

For the logarithmic term, one in fact finds that only the angular integration yields relevant terms:

$$\left\langle \ln\left(\sum_{m=1}^{M}\Delta_m\right)\right\rangle = \frac{1}{\hat{\mathcal{N}}}\int_0^\infty du\,\frac{e^{-\frac{3}{2b^2N}u^2}}{u^{M-1}}\int_0^u d\Delta_1\Delta_1^2\int_0^{u-\Delta_1}d\Delta_2\Delta_2^2\cdots \int_0^{u-\cdots-\Delta_{M-2}} d\Delta_{M-1}\Delta_{M-1}^2(u-\Delta_1-\cdots-\Delta_{M-1})^2 \left(\prod_{m=1}^{M}\int d\Omega_m\right)\ln\left[\Delta_1|\boldsymbol{E}\boldsymbol{e}_1|+\cdots+\Delta_{M-1}|\boldsymbol{E}\boldsymbol{e}_{M-1}| + (u-\Delta_1-\cdots-\Delta_{M-1})|\boldsymbol{E}\boldsymbol{e}_M|\right]$$

with the unit vector $\boldsymbol{e}_m$ specifies the (arbitrary) orientation of the corresponding tube segment $\boldsymbol{\Delta}_m$. Then, one observes

$$\ln\left[\Delta_1|\boldsymbol{E}\boldsymbol{e}_1|+\cdots+\Delta_{M-1}|\boldsymbol{E}\boldsymbol{e}_{M-1}| + (u-\Delta_1-\cdots-\Delta_{M-1})|\boldsymbol{E}\boldsymbol{e}_M|\right] = \ln[u]+\ln\left[|\boldsymbol{E}\boldsymbol{e}_M|\right]+\ln\Bigg[1+\underbrace{\sum_{m=1}^{M-1}\left(\frac{|\boldsymbol{E}\boldsymbol{e}_m|}{|\boldsymbol{E}\boldsymbol{e}_M|}-1\right)\frac{\Delta_m}{u}}_{\text{small since } u\gg|\boldsymbol{\Delta}_m|}\Bigg] \approx \ln[|\boldsymbol{E}\boldsymbol{e}_M|]+\text{const.}$$

In case of uniaxial deformation, the evaluation of $\mathrm{Tr}(\boldsymbol{E}^\top\boldsymbol{E})$, $\overline{|\boldsymbol{E}|}$, and $\overline{\ln|\boldsymbol{E}|}$, cf. eqs 28–30, has been given elsewhere,[14] but for completeness we state them here as well:

$$\mathrm{Tr}(\boldsymbol{E}^\top\boldsymbol{E}) = \lambda^2+\frac{2}{\lambda} \tag{61}$$

$$\overline{|\boldsymbol{E}|} = \frac{1}{2}\left(\lambda+\frac{1}{2\sqrt{\lambda}\sqrt{\lambda^3-1}}\ln\left(\frac{\lambda^{3/2}+\sqrt{\lambda^3-1}}{\lambda^{3/2}-\sqrt{\lambda^3-1}}\right)\right) \tag{62}$$

$$\overline{\ln(|\boldsymbol{E}|)} = \ln(\lambda)-1+\frac{\arctan\sqrt{\lambda^3-1}}{\sqrt{\lambda^3-1}}, \tag{63}$$

APPENDIX B: STRESS TENSOR BEFORE STOCHASTIC AVERAGING

Introducing the tensor notation $\boldsymbol{M}$ enables us to write the network stress $\sigma_{\alpha\beta}$ in eq 41 as a series of compact Gaussian path integrals. The tensor consists of two parts: a *diagonal* contribution due to the distribution function $\psi[f_{p\alpha}(t)]$, and the additional part coming from the exponent containing the $\boldsymbol{\Delta}_m'^\top$ factors in eq 41, which are dependent on $\boldsymbol{x}_p(t)$ and thus linear functions of $\boldsymbol{f}_p$. The latter part is only integrated and defined for times $\le t$. This upper limit on time is dealt with by using Heaviside (step) functions. The tensor $\boldsymbol{M}$ can thus be written as:

$$\begin{aligned}\boldsymbol{M}_{qr}^{\gamma\nu}(t',t'') &= A\,\delta(t'-t'')\delta_{qr}\delta_{\gamma\nu} + b\,(\boldsymbol{E}\boldsymbol{E}^\top)^{-1}_{\gamma\nu}\sin[q]\cos[[q]]\sin[r]\cos[[r]] \\ &\quad\times e^{-(t-t')/\tau_q}\,e^{-(t-t'')/\tau_r}\,\Theta(t-t')\Theta(t-t'') \\ &\equiv A\,\boldsymbol{I}+b\,\boldsymbol{B}.\end{aligned} \tag{64}$$

We use shorthand notations for the combinations of material parameters: $A=(2\zeta_\mathrm{R}k_\mathrm{B}T)^{-1}$ and $b=24/(\zeta_\mathrm{R}^2 s_m\ell^2)$. The matrix $\boldsymbol{B}$ depends on the times and the applied strain tensor:

$$\boldsymbol{B} = (\boldsymbol{E}\boldsymbol{E}^\top)^{-1}_{\gamma\nu}\sin[q]\cos[[q]]\times\sin[r]\cos[[r]]e^{-(t-t')/\tau_q}\,e^{-(t-t'')/\tau_r}.$$

Note that the bracket notation defined in eq 42 is used throughout. The linear term involves a vector $\boldsymbol{g}$, determined by the "memory" of the initial condition, cf. eq 48, given by

$$g_\eta^r(t') = \frac{24}{\zeta_\mathrm{R}s_m\ell^2}\sum_{r_1}\sum_{\eta_1}(\boldsymbol{E}\boldsymbol{E}^\top)^{-1}_{\eta_1,\eta}\times\sin[r_1]\cos[[r_1]]\sin[r]\cos[[r]]\times\boldsymbol{E}_{\eta_1\mu}\boldsymbol{x}_{r_1\mu}(0^-)\,e^{-t/\tau_{r_1}}\,e^{-(t-t')/\tau_r}. \tag{65}$$

Having introduced the tensors, we can present eq 41 in all its glory:

$$\sigma_{\alpha\beta}(t) = \frac{\tilde{c}k\mathcal{N}_\psi\,\mathcal{N}_\mathbb{W}}{\left[\det\boldsymbol{E}\boldsymbol{E}^\top\right]^{\frac{1}{2}}}\int_{-\infty}^{\infty}\frac{d\phi}{2\pi}\,e^{i\phi N}\left[\prod_{\tilde{m}=1}^{M}\int_0^N ds_{\tilde{m}}\,e^{-\left(\frac{1}{3}q_0\ell+i\phi\right)s_{\tilde{m}}}\left(\frac{3}{2\pi\ell^2 s_{\tilde{m}\neq m}}\right)^{-3/2}\right] \times\exp\left\{-\frac{4N}{\ell^2 s_m}\sum_r\sum_{\gamma,\nu}\boldsymbol{E}_{\gamma\mu'}\boldsymbol{E}_{\nu\mu'}(\boldsymbol{E}\boldsymbol{E}^\top)^{-1}_{\gamma\nu}\frac{\sin^2[r]\cos^2[[r]]}{\left(r-\frac{1}{2}\right)^2}\,e^{-2t/\tau_r}\right\}$$

$$\left(\sum_{p\neq q=1}^{N}\frac{4\pi}{N\zeta_{\mathrm{R}}}\left(p-\frac{1}{2}\right)\left(q-\frac{1}{2}\right)\left[\frac{\sin[p-q]\cos[[p-q]]}{p-q}+\frac{\sin[p+q-1]\cos[p+q-1]}{p+q-1}\right]\right.$$

$$\times\left\{E_{\alpha\mu}x_{p\mu}(0^{-})e^{-2t/\tau_p}\int_0^t dt'\,e^{-(t-t')/\tau_q}\int[\mathcal{D}f]f_{q\beta}(t')\,e^{-\frac{1}{2}\boldsymbol{f}^{\top}\boldsymbol{M}\boldsymbol{f}-\boldsymbol{g}^{\top}\boldsymbol{f}}\right.$$

$$+E_{\beta\mu}x_{q\mu}(0^{-})e^{-2t/\tau_q}\int_0^t dt'\,e^{-(t-t')/\tau_p}\int[\mathcal{D}f]f_{p\alpha}(t')\,e^{-\frac{1}{2}\boldsymbol{f}^{\top}\boldsymbol{M}\boldsymbol{f}-\boldsymbol{g}^{\top}\boldsymbol{f}}$$

$$\left.+\frac{1}{\zeta_{\mathrm{R}}}\int_0^t dx\int_0^t dy\,e^{-(t-x)/\tau_p}\,e^{-(t-y)/\tau_q}\int[\mathcal{D}f]f_{p\alpha}(x)f_{p\beta}(y)\,e^{-\frac{1}{2}\boldsymbol{f}^{\top}\boldsymbol{M}\boldsymbol{f}-\boldsymbol{g}^{\top}\boldsymbol{f}}\right\}$$

$$+\frac{2\pi^2}{N^2}\sum_p\left(p-\frac{1}{2}\right)^2\left[s_m+\frac{N}{\pi\left(p-\frac{1}{2}\right)}\sin\left[p-\frac{1}{2}\right]\cos\left[\left[p-\frac{1}{2}\right]\right]\right]$$

$$\times\left\{E_{\alpha\mu}E_{\beta\mu}\frac{k_{\mathrm{B}}T}{k_p}\int[\mathcal{D}f]\,e^{-\frac{1}{2}\boldsymbol{f}^{\top}\boldsymbol{M}\boldsymbol{f}-\boldsymbol{g}^{\top}\boldsymbol{f}}\right.$$

$$+\frac{1}{\zeta_{\mathrm{R}}}\int[\mathcal{D}f]\left(E_{\alpha\mu}x_{p\mu}(0^{-})e^{-t/\tau_p}\int_0^t dt'e^{-(t-t')/\tau_p}f_{p\beta}(t')\right.$$

$$\left.+E_{\beta\mu}x_{p\mu}(0^{-})e^{-t/\tau_p}\int_0^t dt'e^{-(t-t')/\tau_p}f_{p\alpha}(t')\right)e^{-\frac{1}{2}\boldsymbol{f}^{\top}\boldsymbol{M}\boldsymbol{f}-\boldsymbol{g}^{\top}\boldsymbol{f}}$$

$$\left.\left.+\frac{1}{\zeta_{\mathrm{R}}^2}\int_0^t dx\int_0^t dy\,e^{-(2t-x-y)/\tau_p}\int[\mathcal{D}f]f_{p\alpha}(x)f_{p\beta}(y)\,e^{-\frac{1}{2}\boldsymbol{f}^{\top}\boldsymbol{M}\boldsymbol{f}-\boldsymbol{g}^{\top}\boldsymbol{f}}\right\}\right),\quad(66)$$

as it looks like after substituting $x_p(t)$, the full solution of the Langevin equation. To compute the stress tensor given by eq 66, we have to find the determinant of $\boldsymbol{M}_{qr}^{\gamma\nu}(t',t'')$ as well as the correct inverse matrix element. For this, we refer the reader to an analogous calculation presented in ref. 15 for the case of a network with no entanglement constraints.

REFERENCES AND NOTES

1. De Gennes, P. G. Scaling Concepts in Polymer Physics; Cornell University Press: Ithaca, 1985.
2. Edwards, S. F.; Doi, M. The Theory of Polymer Dynamics; Clarendon Press: Oxford, 1986.
3. Edwards, S. F. Proc R Soc London A 1976, 351, 397–406.
4. Edwards, S. F. Br Polym J 1977, 6, 140–143.
5. Gaylord, R. J.; Douglas, J. F. Polym Bull 1990, 23, 529–533.
6. Ball, R. C.; Edwards, S. F.; Doi, M.; Warner, M. Polymer 1981, 22, 1010–1018.
7. Higgs, P. G.; Ball, R. C. Europhys Lett 1989, 8, 357–361.
8. Edwards, S. F.; Vilgis, T. A. Rep Prog Phys 1988, 51, 243–297.
9. Han, W. H.; Horkay, F.; McKenna, G. B. Math Mech Solid 1999, 4, 139–167.
10. Heinrich, G.; Helmis, G.; Vilgis, T. A. Kautsch Gummi Kunstst 1995, 10, 689–696.
11. Rubinstein, M.; Panyukov, S.; Macromolecules 2002, 35, 6670–6686.
12. Edwards, S. F. Proc Phys Soc 1967, 92, 513–519.
13. Flory, P. J.; Erman, B. Macromolecules 1982, 15, 800–806.
14. Higgs, P. G.; Gaylord, R. J. Polymer 1990, 31, 70–74.
15. Vandoolaeghe, W. L.; Terentjev, E. M. J Chem Phys 2005, 123, 034902.
16. Wiegel, F. W. Introduction to Path Integral Methods in Physics and Polymer Science, 1st ed.; World Scientific: Philadelphia, 1986.
17. Des Cloizeaux, J.; Jannink, G. Polymers in Solution: Their Modelling and Structure; Clarendon Press: Oxford, 1989.
18. Flory, P. J. Proc R Soc London Ser A 1976, 351, 351–380.

19. Edwards, S. F. Proc Phys Soc 1967, 91, 9–16.
20. Marucci, G. J Polym Sci Polym Phys 1985, 23, 159–164.
21. Deam, R. T.; Edwards, S. F. Philos Trans R Soc London Ser A 1976, 280, 317–353.
22. Colby, R. H.; Rubinstein, M. Macromolecules 1990, 23, 2753–2760.
23. Milner, S. T.; McLeish, T. C. B. Phys Rev Lett 1998, 81, 725–728.
24. Mooney, M. J Polym Sci 1959, 34, 599–604.
25. Treloar, L. R. G. The Physics of Rubber Elasticity; Clarendon Press: Oxford, 1975.
26. Warner, M.; Terentjev, E. M. Liquid Crystal Elastomers; Clarendon Press: Oxford, 2003.
27. Antman, S. S.; Marlow, R. S. Atti Accad Naz SFMN 1982, 70, 256–264.
28. Antman, S. S.; Marlow, R. S. Arch Ration Mech Anal 1991, 116, 257–299.